JOURNAL OF MATERIALS SCIENCE 26 (1991) 2490–2494

The crystallization of diabase glass

V. ŽNIDARŠIČ-PONGRAC, D. KOLAR
J. Stefan Institute, E. Kardelj University, 61000 Ljubljana, Jamova 39, Yugoslavia

The crystallization behaviour of diabase glass at elevated temperatures was studied in samples prepared by melting the diabase rock. DTA and X-ray analyses revealed the crystallization of diopside ($CaO \cdot MgO \cdot 2SiO_2$) at 865 °C and anorthite ($CaO \cdot Al_2O_3 \cdot 2SiO_2$) at 1060 °C. Further, the kinetics of crystallization of diopside were studied. The phenomenological Johnson–Mehl–Avrami equation was used and the exponent $n = 3/2$ determined from the dependency of the volume fraction of the crystal phase (diopside) on time. The activation energy of crystallization of diabase glass 248 kJ mol^{-1} was estimated on the basis of DTA measurements carried out at different heating rates and found to be in good agreement with literature data for similar glass.

1. Introduction

Diabases are volcanic rocks whose chemical composition is very similar to the much more widespread basalts. Mineralogically they are composed of plagioclases and monoclinic piroxenes, accompanied by accessory minerals such as magnetite, biotite, ilmenite, apatite, olivine etc. In industry diabase rocks are used as a raw material for the production of abrasion and corrosion resistant tiles and mineral wool for heat, noise and fire insulation.

In mineral wool application, the crystallization of amorphous fibres impairs their mechanical properties. On the other hand, the literature [1, 2] cites the superior abrasion and chemical resistance of articles made by controlled crystallization of molten basalt. They can be used wherever the transport of material causes mechanical or chemical abrasion.

The aim of the present work is to study the crystallization of diabase glass by revealing the phases that are formed under certain conditions of heat treatment, and to determine some parameters in the kinetic equations that describe the process of glass crystallization.

2. Experimental procedure

Glass samples were prepared by melting ground diabase (chemical composition in Table I) in a corundum crucible placed in a laboratory electric furnace heated to 1450 °C. After 1 h the melt was water quenched, crushed and melted again twice to achieve better homogeneity. The melt was finally cast into a graphite mould and annealed for 1 h at 650 °C in an electric oven. Cylindrical pieces (approximately 4 mm high and 5 mm in diameter) were cut out of the glass plate and used for the studies of crystallization kinetics, as well as for some DTA experiments (determination of the activation energy for crystallization). According to literature data [3] the specific area of the sample affects the mode of crystallization. By using bulk samples volume crystallization prevails over surface crystallization and the resulting effect on a DTA curve is better defined (narrower).

The crystalline phases which were formed during the crystallization of diabase glass were identified by X-ray diffractometry on a Philips PW 1710 diffractometer using CuK_α radiation.

The kinetics of crystallization of diopside in diabase glass were studied by following their time dependent quantity at a chosen temperature. For this purpose a series of samples were heat-treated at 850 °C for the following times: 0 min (the sample was only heated to this temperature and then rapidly quenched), 5, 10, 15, 30 and 60 min. Internal standard X-ray analysis was used for the determination of the quantity of crystal phase. Aluminium (Koch-Light, 99%, particle size 8 to 15 μm) was chosen as an internal standard. The relative intensities of the diffraction lines of Al: $d_{111} = 0.2338$ nm and of diopside: $d_{22\bar{1}} = 0.2991$ nm were measured, and the wt % of diopside in crystallized samples calculated on the basis of a calibration curve. The latter was produced using mixtures of internal standard, synthetic diopside and diabase glass in certain proportions. Synthetic diopside was prepared by crystallization of a glass of diopside ($CaO \cdot MgO \cdot 2SiO_2$) composition.

DTA analyses were performed on a Netzsch, STA 429 thermoanalyser. The preliminary tests were conducted with 200 mg of powdered sample (particle size below 250 μm) and a heating rate of 5 K min^{-1}. For the determination of the activation energy of crystallization, 200 mg of bulk (cylindrical) samples were placed in platinum crucibles, and Al_2O_3 powder added to improve heat transfer between the sample and the sample holder. These experiments were conducted at heating rates of: 2, 5, 10 and 20 K min^{-1}. All DTA experiments were performed in an air atmosphere with Al_2O_3 powder as reference material.

Crystallized samples were examined with a scanning electron microscope (Leitz AMR 1600T), and

0022-2461/91 $03.00 + .12

TABLE I Chemical composition of diabase (source Orahovica, Bosnia) in wt %

SiO_2	44.3
Al_2O_3	16.9
Fe_2O_3	11.2
CaO	7.4
MgO	11.8
TiO_2	1.9
MnO	0.1
$K_2O + Na_2O$	3.0
loss on ignition	3.3

some of them with a transmission electron microscope (JEM JEOL 2000 FX). Crystals formed in the early stages of crystallization were identified by means of electron diffraction.

3. Results and discussion

3.1. Crystalline phases

The DTA curve of diabase glass (Fig. 1) shows a slope change in the glass transition temperature range (680 °C), two exothermic peaks (865 and 1060 °C) characteristic of crystallization, and a strong endotherm at 1190 °C when melting occurs.

The appearance of two crystallization peaks on a DTA curve implies that at least two different crystal phases are formed during the heat treatment. This was confirmed by X-ray diffraction analysis. The diffraction pattern of a sample heat treated 2 h at 900 °C is shown in Fig. 2. The lines belong to diopside ($CaO \cdot MgO \cdot 2SiO_2$). This phase is accompanied by anorthite ($CaO \cdot Al_2O_3 \cdot 2SiO_2$) at higher temperatures, as shown in Fig. 3. The latter sample was heat treated 2 h at 1100 °C.

3.2. The kinetics of diopside crystallization

Solid state reactions such as the crystallization of glass can be described by the phenomenological Johnson–Mehl–Avrami (JMA) equation [4–9]:

$$X = 1 - \exp[-(kt)^n] \qquad (1)$$

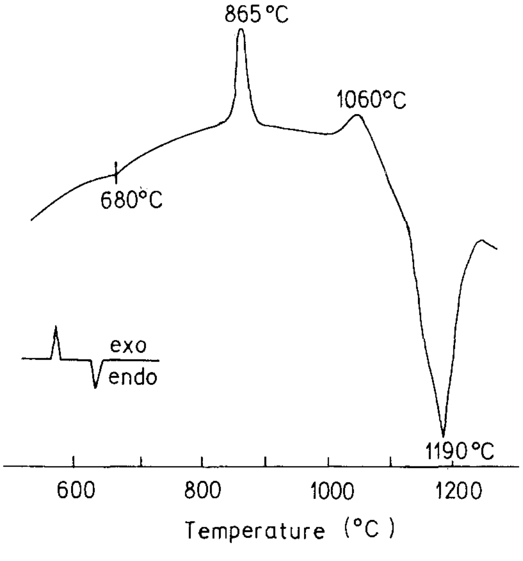

Figure 1 DTA diagram of diabase glass.

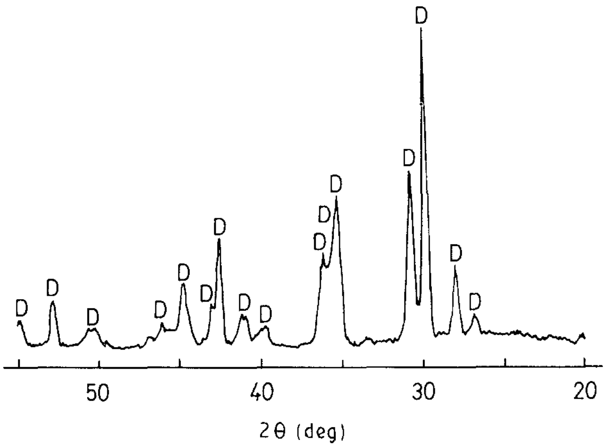

Figure 2 X-ray diffraction pattern of a sample crystallized at 900 °C for 2 h.

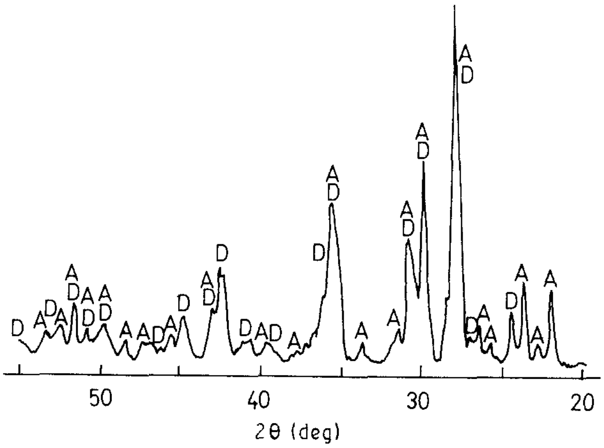

Figure 3 X-ray diffraction pattern of a sample crystallized at 1100 °C for 2 h. (D diopside, A anorthite)

TABLE II Most probable reaction mechanisms and the corresponding values of parameter *n* [6]:

Reaction mechanism	*n*
Crystal growth controlled by interface	
constant nucleation rate	4
constant number of nuclei	3
Crystal growth controlled by diffusion	
constant nucleation rate	5/2
constant number of nuclei	3/2

where X is the volume fraction crystallized after time t, n a dimensionless parameter related to the reaction mechanism as shown in Table II, and k the reaction-rate constant (s^{-1}), whose temperature dependence is generally expressed by the Arrhenius equation

$$k = \nu \exp\left(-\frac{E_a}{RT}\right) \qquad (2)$$

where ν is a frequency factor (s^{-1}), E_a the activation energy for crystallization ($J\,mol^{-1}$), R the gas constant ($8.314\,J\,K^{-1}\,mol^{-1}$) and T the absolute temperature (K).

Taking natural logarithms and rearranging Equation 1 we obtain

$$\ln[-\ln(1 - X)] = n \ln k + n \ln t \qquad (3)$$

From the dependence of $\ln[-\ln(1-X)]$ with $\ln t$ the exponent n can be determined, which is characteristic of the reaction (crystallization) mechanism.

Table III lists data on the fraction of the crystal phase (diopside) as a function of time at 850 °C. Data obtained by means of quantitative X-ray diffraction (wt % diopside) were recalculated into vol % diopside (X in Equation 3). The plot of $\ln[-\ln(1-X)]$ against $\ln t$ is given in Fig. 4, while Figs 5, 6, 7 and 8 show the corresponding microstructures.

Fig. 5 shows a sample of diabase glass heated to 850 °C and rapidly quenched. A great number of crystals approx. 0.1 μm in diameter can be seen. X-ray powder diffraction of this sample does not reveal the presence of diopside; only two weak lines belonging to magnetite (Fe_3O_4) appear.

Fig. 9 is a transmission electron micrograph of the same sample. The crystals whose morphology is still not completely formed are approximately 50 nm in diameter. The electron diffraction pattern (Fig. 10) confirms that they are magnetite crystals.

Fig. 6 shows the sample heat treated for 5 min at 850 °C. Crystals having very fine structure are identified as diopside by X-ray diffraction. The X-ray peaks of diopside and magnetite are partly overlapping, but electron diffraction undoubtedly shows the presence of both phases. Therefore we concluded that the crystallization of diopside in diabase glass proceeds from magnetite nuclei, as was already stated by several authors [1, 10, 11] dealing with a similar (basalt) glass.

The growth of diopside crystals with time is illustrated in Figs 7 and 8.

For the determination of parameter n, we plotted the dependence of $\ln[-\ln(1-X)]$ against $\ln t$ (Fig. 4). As the fraction of diopside remains nearly constant after 30 min at 850 °C, we approximated only the first three points by the least squares method. The slope of the line is

$$n = 1.34 \rightarrow n = 1.5 \text{ or } 3/2$$

TABLE III Fraction of diopside glass as a function of time at 850 °C

Temp./time of cryst. Temperature (°C)	Time of crystallization (min)	Diopside (wt %)	Diopside (vol %)
850	0	—	—
850	5	10	9
850	10	27	24
850	15	36	33
850	30	42	38
850	60	43	39

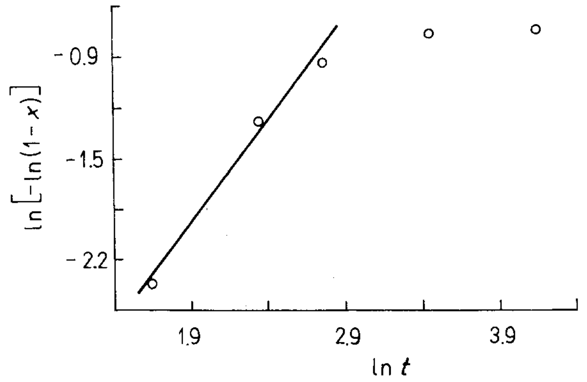

Figure 4 Plot of $\ln[-\ln(1-X)]$ against $\ln t$ for the determination of the parameter n in JMA equation.

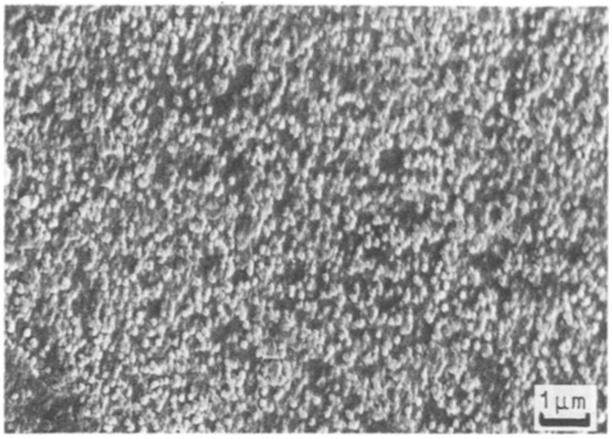

Figure 5 Scanning electron micrograph of a sample heated to 850 °C and rapidly quenched. Polished surface etched with 2.5% HF in ethanol, 30 s.

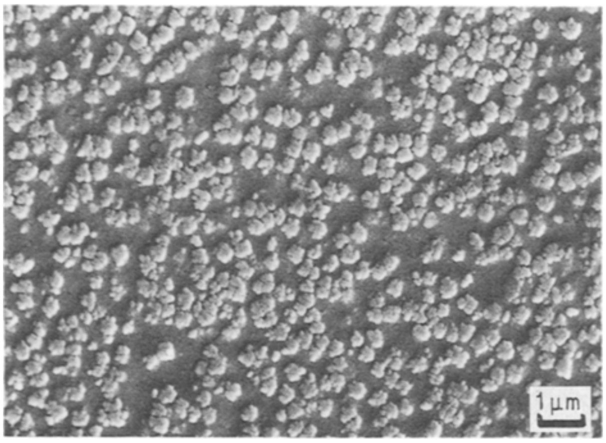

Figure 6 Scanning electron micrograph of a sample heated at 850 °C for 5 min. Polished surface etched with 2.5% HF in ethanol, 30 s.

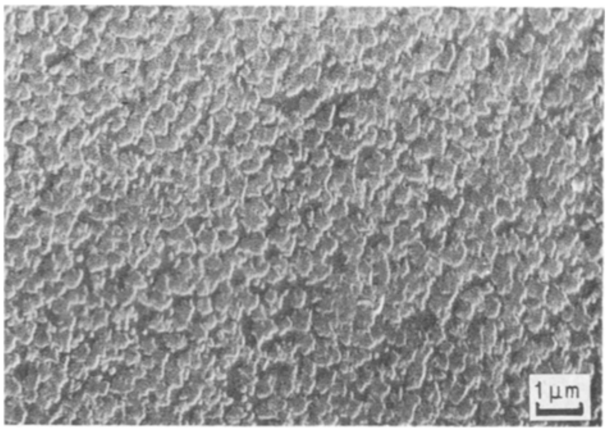

Figure 7 Scanning electron micrograph of a sample heated at 850 °C for 10 min. Polished surface etched with 2.5% HF in ethanol, 30 s.

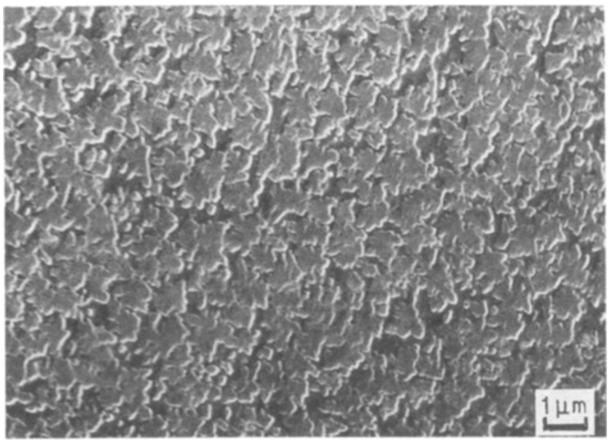

Figure 8 Scanning electron micrograph of a sample heated at 850 °C for 30 min. Polished surface etched with 2.5% HF in ethanol, 30 s.

Figure 9 Transmission electron micrograph of a sample heated to 850 °C and rapidly quenched showing magnetite crystals.

which implies that the growth of diopside crystals at the beginning of crystallization is diffusion controlled and proceeds at a constant number of nuclei. The first of these two statements is logical because the growing crystals have a different composition than the parent glass. The second assumption is partly denied by the comparison of Figs 5 and 6. It seems that part of the originally formed nuclei (subcritical ones) dissolve with time and appear again at a size equal or greater than critical. This phenomenon was also observed by Bandyopadhyay [12], who studied nucleation in basalt glass, and found that the nucleation density diminishes with time at a certain temperature. A fact that gives positive evidence for the constant number of nuclei is the very uniform final microstructure (Fig. 8).

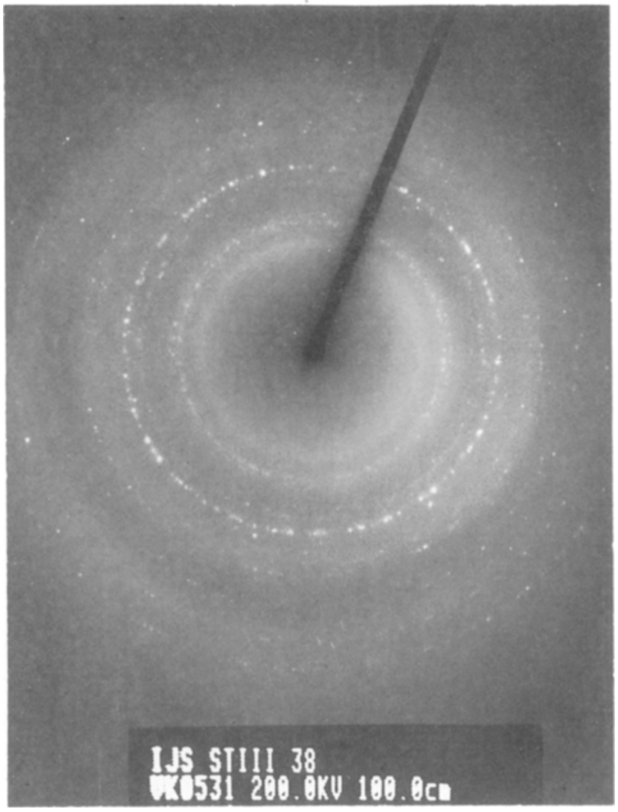

Figure 10 Electron diffraction pattern of the crystal shown in Fig. 9.

3.3. Activation energy for crystallization

The activation energy for crystallization of diabase glass was determined using a method first introduced by Kissinger [13, 14] and modified by several others [15, 16]. This method is based on the dependence of the crystallization peak temperature (T_p) from the DTA heating rate (α) as follows

$$\nu \exp\left(-\frac{E_a}{RT_p}\right) = \frac{E_a \alpha}{RT_p^2} \qquad (4)$$

or in logarithmic form

$$\ln\left(\frac{T_p^2}{\alpha}\right) = \ln\frac{E_a}{R} - \ln\nu + \frac{E_a}{RT_p} \qquad (5)$$

A plot of $\ln(T_p^2/\alpha)$ against $1/T_p$ obtained at various heating rates should be linear with a slope (E_a/R) and the intercept $[\ln(E_a/R) - \ln\nu]$. Therefore, if E_a/R is estimated from the slope, the frequency factor ν can be calculated from the intercept.

Table IV lists data on the variation of the crystallization peak temperature at various heating rates. The same data are graphically plotted in Fig. 11.

In accordance with literature data [17], the temperature of the crystallization peak is higher at faster heating rates. The values of E_a and ν obtained from the slope and the intercept of the line (Fig. 11) are

$$E_a = 248\ \text{kJ mol}^{-1}$$

$$\nu = 2.72 \times 10^{10}\ \text{s}^{-1}$$

The value of E_a is in good agreement with the value reported by Voldan ($E_a = 245\ \text{kJ mol}^{-1}$) [18], who studied the kinetics of crystallization of basalt glass using the isothermal method.

TABLE IV DTA measurements

Heating rate, α ($\mathrm{K\,min^{-1}}$)	Peak temperature, T_p (K)	(°C)
2	1107	(834)
5	1137	(864)
10	1162	(889)
20	1203	(930)

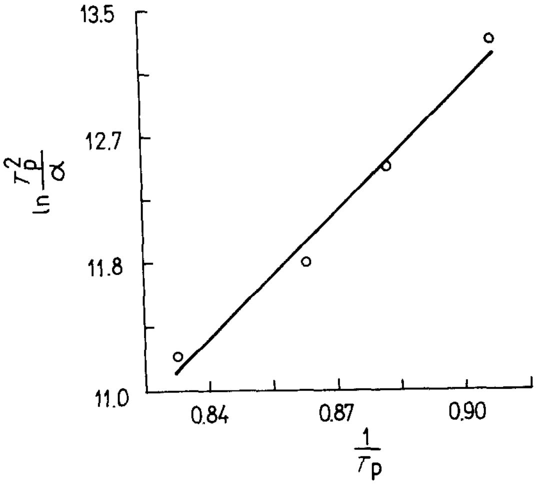

Figure 11 Plot of $\ln(T_p^2/\alpha)$ against $1/T_p$ for the determination of the activation energy for the crystallization of diabase glass.

4. Conclusion

The crystallization of diabase glass is a two-step process. The crystallization peak of diopside on the DTA curve appears at 865 °C, followed by anorthite at 1060 °C. Both phases appear after prolonged heat-treatment at even lower temperatures than those revealed by DTA.

The phenomenological Johnson–Mehl–Avrami equation was used for the description of the kinetics of crystallization and the parameter n was determined by following the time-dependent fraction of crystal phase at 850 °C. The value of n is 3/2, indicating diffusion-controlled growth of crystals at a constant number of nuclei. Scanning and transmission electron analyses of crystallized samples revealed that the growth of diopside crystals proceeds from magnetite nuclei.

The parameters of the Arrhenius equation (E_a, ν) were determined by following the dependence of crystallization peak temperature on DTA heating rate. Their values are $248\ \mathrm{kJ\,mol^{-1}}$ and $2.72 \times 10^{10}\ \mathrm{s^{-1}}$, respectively.

References

1. G. H. BEALL and H. L. RITTLER, *Ceram. Bull.* **55** (1976) 579.
2. A. CROOK and R. E. BEAL, *Mater. Performance* **1** (1980) 45.
3. A. MAROTTA, A. BURI and F. BRANDA, *Thermochim. Acta* **40** (1980) 397.
4. M. AVRAMI, *J. Chem. Phys.* **7** (1939) 1103.
5. *Idem., ibid.* **8** (1940) 212.
6. *Idem., ibid.* **9** (1941) 177.
7. P. HAUTOJÄRVI, A. VEHANEN, V. KOMPPA and E. PAJANNE, *J. Non-Cryst. Sol.* **29** (1978) 365.
8. F. BRANDA, A. BURI, A. MAROTTA and S. SAIELLO, *Verres Refract.* **33** (1979) 201.
9. N. P. BANSAL and R. H. DOREMUS, *J. Amer. Ceram. Soc.* **66** (1983) 233.
10. J. VOLDÁN, *Sklář. Keram.* **30** (1980) 180.
11. M. HIDALGO, P. CALLEJAS and J. MA. RINOON, in "Ceramic Microstructures '86: Role of Interfaces" (Plenum, New York, 1987) pp. 117–126.
12. A. K. BANDYOPADHYAY, P. LABARBE, J. ZARZYCKI and A. F. WRIGHT, *J. Mater. Sci.* **18** (1983) 709.
13. H. E. KISSINGER, *J. Res. Nat. Bur. Stand.* **57** (1956) 217.
14. H. E. KISSINGER, *Anal. Chem.* **29** (1957) 1702.
15. N. P. BANSAL, R. H. DOREMUS, *J. Therm. Anal.* **29** (1984) 115.
16. R. F. SPEYER, S. H. RISBUD, *Phys. Chem. Glasses* **24** (1983) 26.
17. W. Wm. WENDLANDT, in "Thermal Methods of Analysis" (John Wiley, New York, 1974) pp. 178–187.
18. J. VOLDÁN, *Informativní přehled, Státny Výzkumný Ústav Sklářský, Hradec Králové* **15** (1972) 1.

Received 12 February
and accepted 13 August 1990